IEEE Access
Multidisciplinary ⋮ Rapid Review ⋮ Open Access Journal

Received December 19, 2019, accepted January 4, 2020, date of publication January 9, 2020, date of current version January 17, 2020.

Digital Object Identifier 10.1109/ACCESS.2020.2965214

A Novel Method of Soil Parameter Identification and Force Prediction for Automatic Excavation

YUMING ZHAO[1,2,3], JIAN WANG[1,2], YI ZHANG[1,2,4], AND CHAO LUO[3]

[1]School of Mechanical and Electrical Engineering, Central South University, Changsha 410083, China
[2]The State Key Laboratory of High Performance and Complex Manufacturing, Changsha 410083, China
[3]Sunward Intelligent Equipment Company, Ltd., Changsha 410100, China
[4]School of Mechanical and Electrical Engineering, Changsha University, Changsha 410082, China

Corresponding author: Yi Zhang (zhangyicsu@csu.edu.cn)

This work was supported by the Research and Development projects in key areas of Hunan Province under Grant 2019SK2181.

ABSTRACT A shortage of soil property parameters is preventing the automatic excavation system from being used in a digging operation adaptively like an operator. This study proposes a new method of soil parameter identification and digging resistance prediction that classifies the entire excavation process into three parts: penetration, cutting, and loading. A fuzzy estimation strategy is introduced into penetration to estimate the property parameters of the soil depending on the peak value and the average value of soil resistance. Furthermore, an improved FEE model was used to describe the soil–tool interaction and predict the soil resistive forces. The traditional way of predicting after identifying, which needs at least two excavations, can hardly equal this method in flexibility and real-time functionality. The proposed method can identify soil parameters and predict digging forces on one excavation, which is more adapt to soil parameter variation. The experimental results show that the proposed method can identify precisely and predict effectively.

INDEX TERMS Excavation, soil parameter identification, force prediction.

I. INTRODUCTION

The hydraulic excavator, a multi-functional machine that has been extensively used in earth-moving industries such as infrastructure construction, mining, and agriculture, is a type of multi-axis system that depends on operator experience to realize improved coordinate motion. Efficiency and quality of excavation processing suffer and equipment aging accelerates when no skilled operators are present or fatigued driving occurs, which is a safety problem. However, the training of a professional operator is time-consuming and costly. Thus, to address these problems, researchers have proposed the concept of hydraulic excavator automation [1]–[4].

Most of the literature focuses on the planning and control of excavator systems [5], [6]. The influence of soil resistance on excavation work is not considered, which causes difficulty for the automatic excavation system but is favorable for an operator in planning the operation trajectory and completing the excavation according to the soil properties. Modeling the soil–tool interaction and predicting resistive forces can make up for this deficiency [7]. The predicted forces can be used in digging strategy and excavator simulation systems with better performance because the former avoids overloading that may damage the machine [8], while the latter improves the accuracy of the excavation process model [9]. Depending on the predicted resistance, we can improve the excavation strategy, plan the excavation trajectory [10], and design a suitable controller for trajectory tracking control [11]. In other words, the key to promote excavator automation quality lies in the efficiency of soil property identification and resistance prediction of the bucket [12].

Two challenges remain in the prediction of soil–tool interaction force: one is obtaining the soil parameters and the other is establishing the soil resistance prediction model. For the first challenge, Luengo *et al.* [13] used a combination of exhaustive search and gradient descent search to extract soil parameters based on fundamental earthmoving equation (FEE). Won used the parameter space intersection method (PSIM) to estimate soil parameters, but improving the accuracy is difficult [14]. Using the CLUB and Mohr-Coulomb models, Althoefer *et al.* used the Newton–Raphson method to identify soil properties but identified only two parameters [15]. In the study by Kim, the identification of soil parameters is expressed as an optimization problem [10].

The associate editor coordinating the review of this manuscript and approving it for publication was Xiao-Sheng Si.

This approach often requires a large amount of calculation and time, which is not conducive to real-time applications. On the other hand, to accurately predict the excavation resistance, many researchers are working on the improvement of the soil–tool interaction model. Using the fundamental earthmoving equation proposed by Reece [16], Mckey established a relatively complete model of soil–tool interaction, which includes soil cohesion, friction, additional force, and inertial force [17]. Similarly, Zeng *et al.* established a soil resistance model based on the principle of soil mechanics and applied it to predict the resistive force of lunar soil collection [18]. Furthermore, Zou added the soil inertial force to Park's model [19] and used it to predict excavation resistance and trajectory planning [20]. Among these models, the FEE model proposed by Reece is considered as a classic model for soil–tool mechanical analysis and is widely used in soil resistance prediction [9], [14].

When the bucket penetrates the soil at the beginning of excavation work, the skilled operator can judge the hardness of the soil depending on the force feedback and adjust the dig trajectory to avoid excessive resistance and improve the excavation efficiency. In this study, we imitate manual operation and propose a novel method for predicting the excavation resistance. Unlike the traditional prediction-after-identification method that needs at least two excavations, the new methods can complete parameter identification and resistance prediction in a one-time excavation. First, soil property parameters are identified based on the characteristics of the force when the bucket penetrates the soil; we use a fuzzy-rule-based identification method. To the best of our knowledge, this study represents the first time that fuzzy methods are applied to soil parameter identification. Furthermore, an improved FEE model was used to describe the soil–tool interaction and predict the soil resistive forces. Compared with the existing methods, the proposed parameter identification method does not depend on the accurate mathematical models and is simple and time-saving to implement, which is beneficial for practical applications. This method is also more adaptable for changing soil parameters because we can perform dynamic soil parameter identification and prediction of excavation resistance during each excavation process.

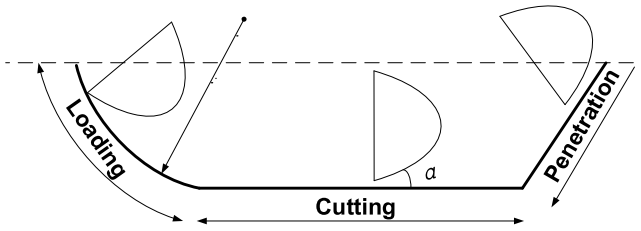

FIGURE 1. Three stages of the excavation process.

II. PROBLEM DESCRIPTION

As shown in Fig. 1, the entire excavation process can be divided into three stages according to the movement states of the bucket: penetration, cutting, and loading [21]. During the penetration phase, the bucket begins to cut into the soil with a set angle until the end of the bucket drops to a certain depth. Then, the soil is cut and loaded into the bucket at the cutting stage. For simplicity, this study only considers that the bucket moves linearly in the horizontal direction during cutting. Finally, the joints cooperate to lift the bucket and the soil in the loading phase.

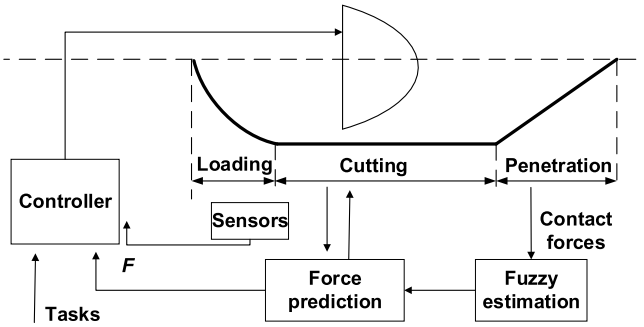

FIGURE 2. Soil parameter identification and resistance prediction framework.

The framework of our proposed automatic excavation system is shown in Fig. 2. The system consists of four parts: signal acquisition, fuzzy estimation, resistance prediction, and control. During penetration, the pressure data are collected by the oil pressure sensors installed on the cylinders, and then the soil resistive forces are calculated through dynamics, which are the inputs of the fuzzy estimation module. Then, according to the established fuzzy database and fuzzy rules, the hardness of the soil is judged by the fuzzy method, and the soil property parameters are estimated. Moreover, the soil parameters and bucket posture are used as inputs of the force prediction module. We use the improved FEE model proposed by Singh [22] to calculate soil resistance during cutting. Furthermore, the predicted force can be utilized for trajectory optimization and controller design.

III. FUZZY IDENTIFICATION OF SOIL PARAMETERS (PENETRATION STAGE)

A. ANALYSIS OF RESISTANCE CHARACTERISTICS

Although penetration and cutting during the excavation are two different actions, the forces observed during cutting have the same properties as those in penetration [23]. In addition, in practice, some scholars have used penetrating devices as a measure of cutting resistance [21]. As the soil resistance during penetration is related to the soil properties, those force characteristics are used to identify soil parameters in this study. For penetration, many researchers have established empirical models based on experimental results with no versatility [24]. Furthermore, using the cavity expansion theory, Park established a resistance prediction model when the bucket penetrated the soil [19]. This model was used for soil resistance prediction in the study by Bennett *et al.* [9] and Zou *et al.* [20]. However, due to the complexity of this model and the inability to reverse the soil parameters from

the force, directly using this model to identify soil parameters is difficult. As the mechanism model for the penetration is difficult to establish and the model is complex, the model-based identification method normally requires a large amount of calculation and time and is not conducive to practical application in engineering, which is also the motivation for us to identify the soil parameters using fuzzy methods. These fuzzy rules do not depend on the mathematical model or any complex calculation [25], and the soil property parameters can be identified quickly.

To verify the relationship between forces during penetration and the hardness of the soil, as shown in Fig. 3, five types of soil were loaded into large containers and normalized penetration actions were completed. These five types of soil are sand, Clayey sand, Loam, Silt loam, and Heavy clay, the parameters of which were tested by professional instruments. As shown in Table 1, the hardness and soil property parameters are positively correlated with each other.

FIGURE 3. Experiment site of soil penetration test.

TABLE 1. Soil parameters.

Names	γ (kg/m^3)	c (kPa)	δ $(^\circ)$	ϕ $(^\circ)$
Sand	1604	1.0	21.8	25.2
Clayey sand	1682	7.1	24.2	26.3
Loam	1753	13.2	28.4	32.0
Silt loam	1839	16.4	25.6	33.7
Heavy clay	2163	24.7	30.1	34.6

As the movement postures of the bucket have a great influence on the soil resistive forces during excavation, this study ensures that the postures and speed of the bucket are the same when digging different soil types. The bucket tip trajectory during the penetration test is shown in Fig. 4, where depth $H = 0.3$ (m) and dig angle $\alpha = 40^\circ$. During these experiments, the pressures of the hydraulic cylinder collected by the pressure sensors are shown in Fig. 5. We only show the sand digging test data similar to the pressure values of other experiments. Furthermore, the dynamics of the excavator were used to calculate soil-bucket interaction forces. The forces of the five groups of the penetration test are shown in Fig. 6. The experimental results show that the harder the soil is, the greater the soil resistance becomes. That is, the penetration resistance can reflect the nature of the soil, which is why an experienced excavator operator can roughly judge the hardness of the soil through force feedback at the beginning of each excavation. Imitating the manual operation, we propose a novel method for obtaining soil hardness and estimating soil parameters based on the resistive forces during the penetration stage. The entire process is shown in Fig. 7.

B. FUZZY ESTIMATION

The fuzzy estimation model of soil parameters proposed in this paper is based on a resistance database that consists of a large number of soil resistance experimental data in the penetration stage. The specific process is shown in Fig. 8, where the resistance characteristic is the input of the fuzzy estimation model, and the soil parameter values are obtained by defuzzification and transformation.

As shown in Fig. 6, the peak values of the five resistance curves are positively related to the soil hardness, specifically, contact force increases as the soil become harder. Therefore, the fuzzy system takes the maximum value of resistance F_{max} and the average value of resistance F_{avg} as inputs, and the expressions are as follows:

$$F_{avg} = \frac{1}{N}\sum_{n=1}^{N} F_s \tag{1}$$

where F_s is the interaction force between the bucket and the soil of every sample time, and N is the number of samplings. According to the experimental database, the peak resistance varies from 0 to 6kN, and the range of the average forces is confined to [0,3.2kN] in approximately 3 s.

For convenience, F_{max} and F_{avg} are normalized to the range between zero and one by the linear transformation. The fuzzy inputs E and R of the system are obtained by multiplying the quantization factors k_1 and k_2, respectively, and the physical domains are changed into the fuzzy sets. Input and output membership functions use triangular membership functions. As shown in Fig. 9 (a), (b), input information F_{max} and F_{avg} are defined as five fuzzy sets: very small (VS), small (SL), medium (ME), relatively large (RL), large (LE). The output of the fuzzy estimation is soil hardness k_d, which indicates the magnitude of resistance to excavation. As shown in Fig. 9 (c), it is also defined as five fuzzy sets: very soft (VS), medium soft (MS), medium (ME), penetration (MH), and very hard (VH). E is A_i and R is B_j, then $\tilde{f}$ is G_{i+j}, where E and R, A_i and B_j denote input variables and input fuzzy sets, respectively; $\tilde{f}$ and G_{i+j} denote the estimating force and output fuzzy set, respectively. The details of the rules are shown in Table 2.

The inference adopts a standard Mandani inference engine. The center of sets method is used to obtain a crisp output [26],

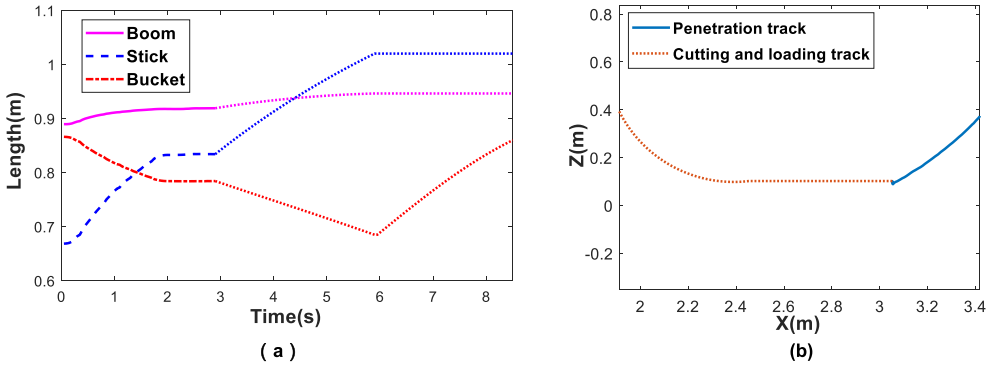

FIGURE 4. Cylinder length and bucket tip trajectory during penetration a) Cylinder length. b) Bucket tip trajectory.

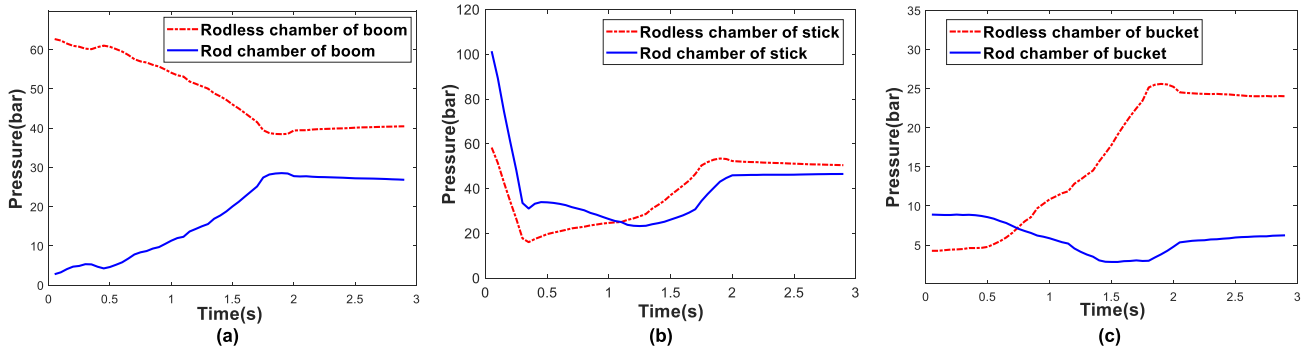

FIGURE 5. Cylinder pressures during sand penetration test a) Boom. b) Stick. c) Bucket.

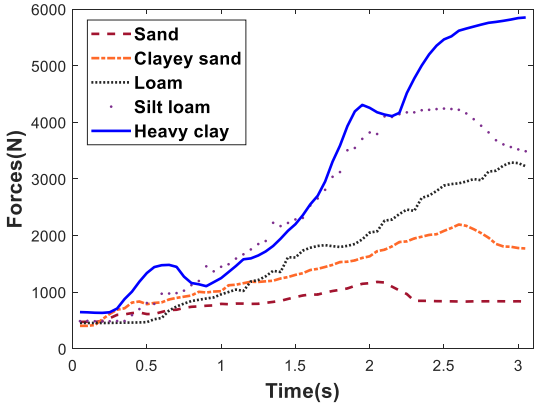

FIGURE 6. Soil resistive forces during penetration.

TABLE 2. Fuzzy reasoning rules.

k_d		F_{max}				
		HB	HS	MK	SS	SB
F_{avg}	HB	HB	HB	HS	MK	SS
	HS	HB	HS	MK	MK	SS
	MK	HB	HS	MK	SS	SB
	SS	HS	MK	MK	SS	SB
	SB	HS	MK	SS	SB	SB

which is

$$k_d = \frac{\sum_{m=1}^{M} g^m \left[\mu_{A_1^m}(F_{\max}) * \mu_{B_T}(F_{\alpha_g})\right]}{\sum_{m=1}^{M} \left[\mu_{A_1^n}(F_{\max}) * \mu_{B_j^2}(F_{\alpha_Z})\right]} \quad (2)$$

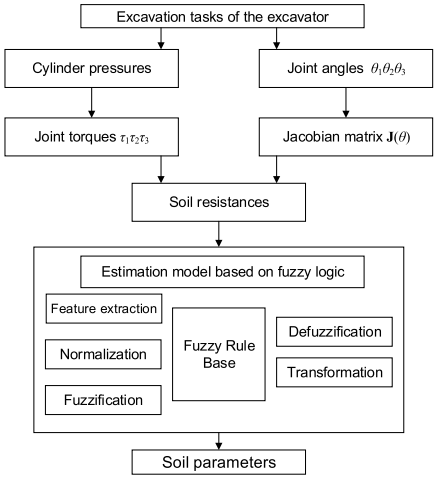

FIGURE 7. Online soil parameter identification process.

where g^m is the centroid of the consequent set of the mth fired rule, M denotes the number of fired rules, $\mu_{A_i^l}(F_{\max})$ and $\mu_{B_j^l}(F_{avg})$ respectively denote the membership functions of input F_{avg} and F_{max}, and $*$ denotes the t-norm operator.

C. SOIL PARAMETER ACQUISITION

The output of the fuzzy model, k_d, can be obtained in each soil penetration test. After the five sets of experiments, the ranges and average values of k_d are shown in Table 3. The range of k_d

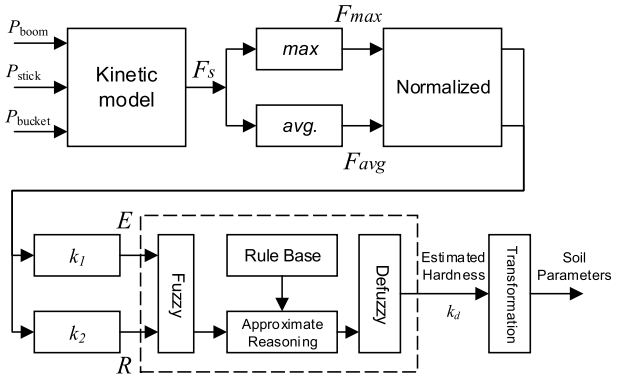

FIGURE 8. Fuzzy estimation model.

TABLE 3. Hardness of soil.

names	k_{dmin}	k_{dmax}	k_d
Sand	0.181	0.211	0.196
Clayey sand	0.374	0.445	0.410
Loam	0.509	0.606	0.558
Silt loam	0.641	0.792	0.717
Heavy clay	0.879	1.000	0.940

values approaches 0.2, while k_d of the Heavy clay is close to the maximum value. The values of k_d, which are positively correlated with the soil parameters, can be used to indicate the soil hardness. To obtain the soil parameters, k_d was used as the independent variable, the known soil parameters (soil parameter values are shown in Table 1) are regarded as the dependent variables, and the least-squares method [27] was used to fit equations (3)-(6).

$$\gamma = 4201.9 \times K_d^4\text{-}7540 \times K_d^3 + 4910 \times K_d^2 - 963.7 \times K_d + 1652.3 \quad (3)$$

$$c = 584.7 \times K_d^4\text{-}1303.7 \times K_d^3 + 997 \times K_d^2 - 272.4 \times K_d + 25.1 \quad (4)$$

$$\delta = 972.8 \times K_d^4\text{-}2152 \times K_d^3 + 1629 \times K_d^2 - 479.6 \times K_d + 68.2 \quad (5)$$

$$\phi = 637.7 \times K_d^4\text{-}1539 \times K_d^3 + 1281 \times K_d^2 - 408.72 \times K_d + 67 \quad (6)$$

IV. MODELING OF SOIL-BUCKET INTERACTION FORCE CUTTING

A. IMPROVED FEE MODEL

During the cutting phase, the bucket can be simplified into a baffle that pushes the soil and accumulates it in the bucket. This process is subject to large soil forces that affect the efficiency and energy consumption of earthmoving. Therefore, we mainly analyze the soil–tool interaction during the cutting stage and establish a force prediction model in this study. In general, the calculation of soil excavation forces becomes complicated due to the difficulty in obtaining accurate characteristics of the soil. The selection of soil–tool interaction models can seriously affect the accuracy and performance of dig force prediction [28]. For this study, the improved FEE model proposed by Singh [22] is selected.

The FEE model assumes that the cutting plate moves forward under external force, and the soil is cut along the failure surface by the cutting plate to form a soil wedge. This process is similar to the process of cutting the soil by an excavator. According to the literature [10], the static force analysis of the soil wedge model under inclined terrain is shown in Fig. 10. Where α is terrain slope. Lt is the length of the tool, Lf is the length of the surface along which the wedge slides, Q is the surcharge (or the displaced soil that rests on the wedge), φ is the soil–soil friction angle, c is the cohesiveness of the soil, ca is the adhesion between the soil and blade, δ is the soil–tool friction angle, R is the force of the soil resisting the movement of the wedge, and F is the force exerted by the tool to cause failure. The material in the shaded region constitutes all of the material that has passed over the top of the bucket tip during the motion of the bucket, and *Vs* is referred to as the swept volume.

The model calculates the soil–tool interaction force based on the following soil parameters:

δ: the angle between the bucket blade and soil force F,
ϕ: the angle between the failure plane and resistive force R,
β: the angle between the terrain surface and failure plane,
γ: mass density of the soil,
c: soil cohesion parameter.

The soil resistance to the bucket F_{soil} can be calculated by

$$F_{soil} = w\gamma g d^2 N_\gamma + wcdN_c + V_s\gamma g N_q \quad (7)$$

$$\angle F = \frac{\pi}{2} - \rho - \delta \quad (8)$$

where

$$N_\gamma = \frac{(\cot\beta - \tan\alpha)[\cos\alpha + \sin\alpha\cot(\beta+\phi)]}{2[\cos(\rho+\delta) + \sin(\rho+\delta)\cot(\beta+\phi)]}$$

$$N_c = \frac{1 + \cot\beta\cot(\beta+\phi)}{\cos(\rho+\delta) + \sin(\rho+\delta)\cot(\beta+\phi)}$$

$$N_q = \frac{\cos\alpha + \sin\alpha\cot(\beta+\phi)}{\cos(\rho+\delta) + \sin(\rho+\delta)\cot(\beta+\phi)}$$

We note that Γ = (d,w,α, ρ,Vs) is the geometrical parameter of the bucket during the excavation process, corresponding to the depth of the top of the bucket, the width of the bucket, slope of the terrain, cutting angle, and swept volume. Once we know the attitude, shape, and topography of the bucket, we can calculate Γ = (d,w,α, ρ,Vs), which can be considered a known parameter in this study.

B. EXCAVATOR DYNAMICS INCLUDING SOIL RESISTANCE

As the soil–tool interaction force cannot be directly measured, we installed the oil pressure sensors on the hydraulic cylinder to collect the pressure data during excavation. Then, the soil resistance could be calculated through the excavator dynamics; thus, we have to establish a dynamic model of the excavator robot arm. Without the rotation of the upper

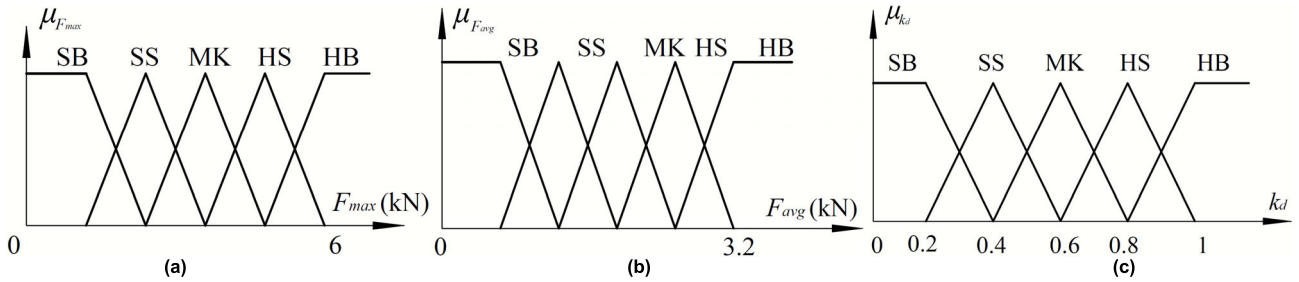

FIGURE 9. Membership functions of fuzzy methods (a) F_{max} (b) F_{avg} (c) k_d.

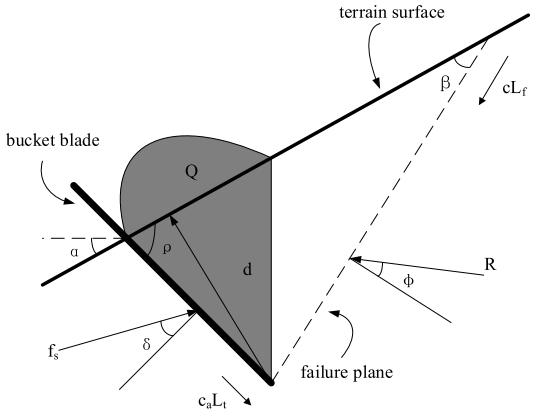

FIGURE 10. Improved FEE model.

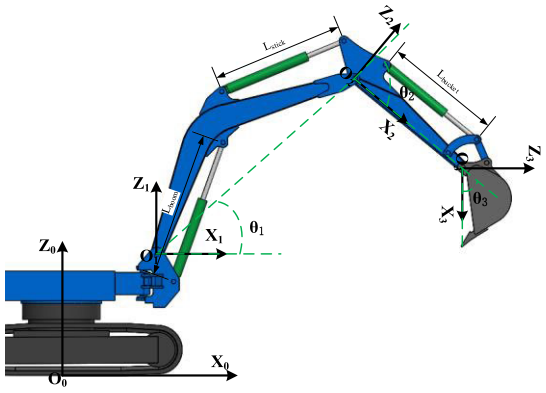

FIGURE 11. D-H coordinates of excavator.

platform, the D-H coordinates of the 3-DOF manipulator are shown in Fig. 11, and the dynamic equation is expressed as

$$\boldsymbol{\tau} = \mathbf{M}(\boldsymbol{\theta})\ddot{\boldsymbol{\theta}} + \mathbf{C}(\boldsymbol{\theta}, \dot{\boldsymbol{\theta}})\dot{\boldsymbol{\theta}} + \mathbf{G}(\boldsymbol{\theta}) + \mathbf{J}^{\mathrm{T}}\mathbf{F} \tag{9}$$

where $\boldsymbol{\theta}, \dot{\boldsymbol{\theta}}, \ddot{\boldsymbol{\theta}}$ are the 3×1 vectors of joint position, velocity, and acceleration; $\mathbf{M}(\boldsymbol{\theta})$ is the 3×3 inertia matrix; $\mathbf{C}(\boldsymbol{\theta}, \dot{\boldsymbol{\theta}})$ is the 3×1 Coriolis and centripetal matrix; $\mathbf{G}(\boldsymbol{\theta})$ is the 3×3 vector of gravity terms; $\boldsymbol{\tau} = [\tau_1, \tau_2, \tau_3]^{\mathrm{T}}$ is the vector specifying the torques acting on the joint shafts (for the excavation robot studied in this paper, it can be obtained by measuring the driving force of the hydraulic cylinder); $\mathbf{J}$ is a 3×3 Jacobian

TABLE 4. Soil parameters for model verification test.

Parameter and symbol	Value
Density (γ)	1598kg/m^3
Cohesion (c)	0.4kPa
Bucket-soil friction angle (δ)	22.1°
Internal friction angle (ϕ)	25.2°

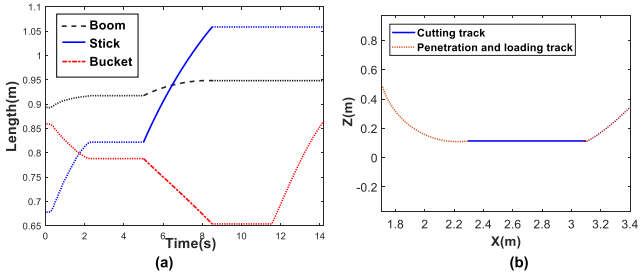

FIGURE 12. Cylinder length and bucket tip trajectory during the verification test (a) cylinder length (b) bucket tip trajectory.

matrix, and $\mathbf{F}$ is external load force. Thus, we obtain:

$$F = \begin{bmatrix} F_{soil} \cdot \cos \angle F \\ F_{soil} \cdot \sin \angle F \\ F_{soil} \cdot \cos \angle F \cdot L4 \cdot \sin \psi + F_{soil} \cdot \sin \angle F \cdot L4 \cdot \cos \psi \end{bmatrix}$$

As the speed and acceleration of the manipulator during the excavation process are small, their influences on the dynamics can be neglected, so the soil resistance can be calculated by the following formula:

$$\mathbf{J}^{\mathrm{T}}\mathbf{F} = \tau - \mathbf{G}(\boldsymbol{\theta}) \tag{10}$$

C. MODEL VERIFICATION

A field test of the digging process has been conducted to verify the fidelity of the improved FEE model. Soil parameters for the digging test are presented in Table 4. The experiment was tested according to a typical excavation trajectory as mentioned, and the bucket tip trajectory generated in the experiment is shown in Fig. 12. The dig angle $\alpha = 40°$, the vertical depth $H = 0.3$ (m), and the horizontal moving distance L = 0.5(m).

The pressure of each chamber of the hydraulic cylinders obtained in the experiment is shown in Fig. 13, and the

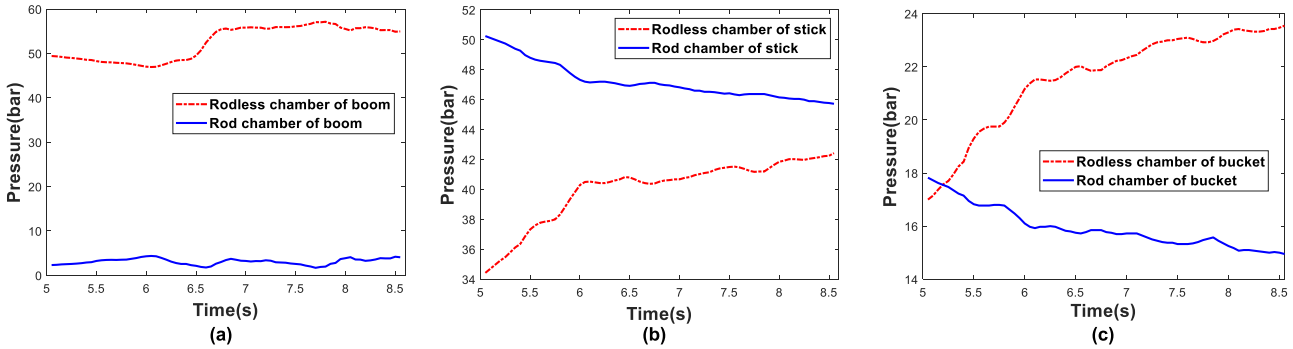

FIGURE 13. Cylinder pressures during the verification test (a) Boom. (b) Stick. (c)Bucket.

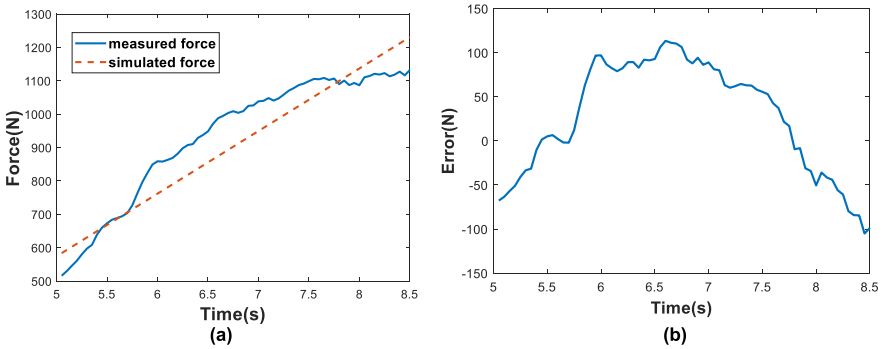

FIGURE 14. Simulated forces and measured soil forces during the verification test (a) Comparison. (b) Error.

driving force of the hydraulic cylinder can be calculated by the following formula:

$$Fi = P1i \cdot A1i - P2i \cdot A2i, i = boom, stick, bucket \quad (11)$$

where $P1i$, $P2i$ is the pressure of the rodless and rod chambers, and $A1i$, $A2i$ is the effective working area.

The actual soil resistance during the cutting stage is obtained through the dynamics of the excavator. Furthermore, the improved FEE model is used to predict the soil–bucket interaction force during 3cutting. The prediction forces and measured forces are compared in Fig.14 (a), and Fig.14 (b) shows the prediction error. Although the comparison results show discrepancies, using the improved FEE model to simulate the cutting process of an excavator is still promising because the simulated soil forces show relatively good agreement with measured forces in the overall trends.

V. EXPERIMENTS

A. EXPERIMENT PLATFORM

The experimental platform is based on the SUNWARD-SWE17 hydraulic excavator, as shown in Fig. 15. To complete the experiment conveniently, we place the soil into a box for the test.

Fig. 8 shows the architecture of the entire experimental platform where the entire system is divided into a slave part and a master part, which are connected through the CAN bus (CANpro II, China). The slave part is based on a 1.7-ton hydraulic excavator (SUNWARD-SWE17, China). In addition, sensors and a DSP controller are installed to collect data during the excavation test.

Draw-wire displacement transducers (WXY33-1212, China) are installed on the hydraulic cylinders to measure the piston displacements of boom, stick, and bucket, and then kinematics are used to obtain the position of the bucket tip. Besides, six-cylinder pressure sensors (IFM-PT5500, Germany) are mounted on the joints of the corresponding cylinders to measure the oil pressure of the rod and rodless chambers. The slave part uses the DSP controller (SUNWARD-SWMC3, China) for data acquisition, data transmission, and trajectory tracking control. The controller can convert the analog signal of the sensors into digital signals, which are sent to the master part through the CAN bus. For the master part, based on the MATLAB GUI environment, the host computer realized data reception, data storage, display, soil parameter identification, and force prediction.

In order to satisfy the real-time application, a fuzzy control table is established. Using the table lookup method to realize fuzzy estimation can save CPU operation time and improve efficiency. In the experiments, the sampling time of the system is about 20ms, and the fuzzy estimation method can complete the identification of soil parameters within 1 or 2 sampling intervals.

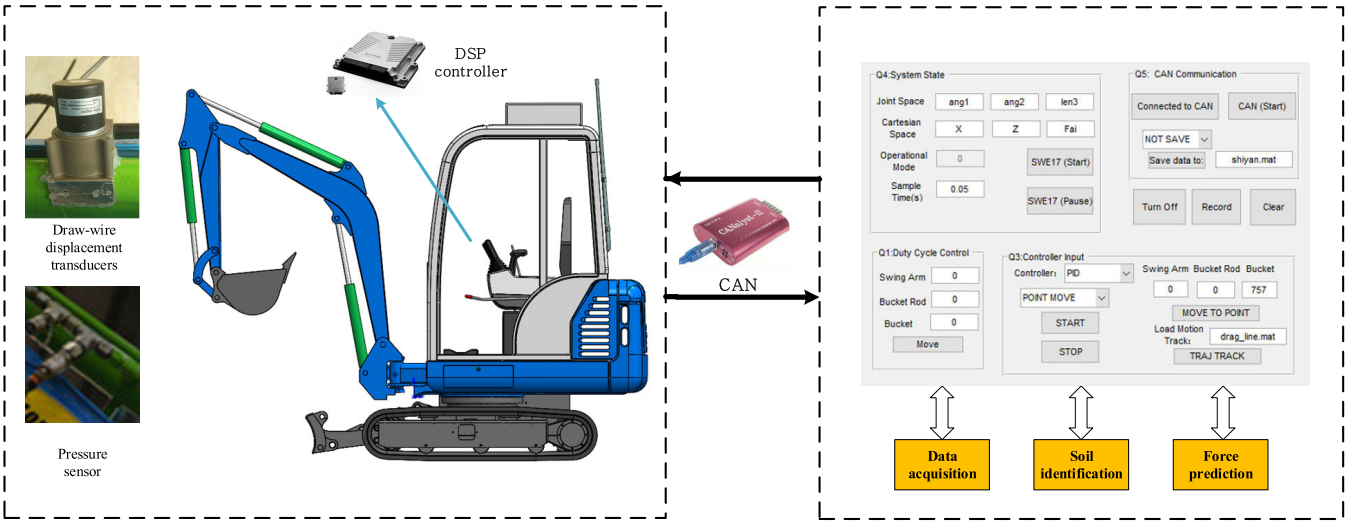

FIGURE 15. Experimental platform.

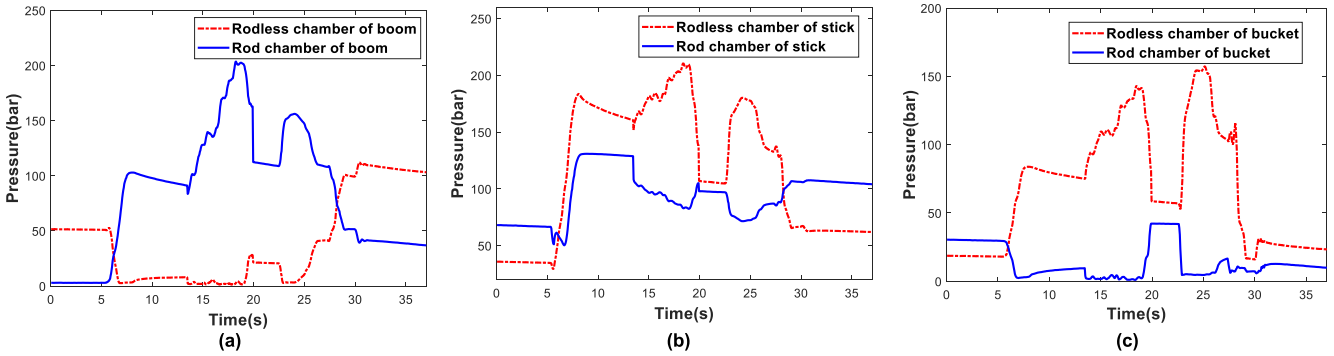

FIGURE 16. Cylinder pressures during Test 1 (a) boom (b) stick, (c)bucket.

B. TEST 1 (SOIL WITH KNOWN PARAMETERS)

Having established the proposed framework for soil parameter identification and soil-bucket interaction forces prediction, we now examine its capabilities in the actual excavation process. In the third section, five types of soil are used to establish the fuzzy rule library, which is the basis for identifying the soil parameters. We select sand as the experimental soil to verify the effectiveness of the proposed methods. The parameters of the sand are listed in Table 1. The test is still performed using the typical excavation trajectory shown in Fig. 4(b) and Fig. 12(b), the dig angle $\alpha = 40°$, the vertical depth $H = 0.25$ (m), and the horizontal moving distance $L = 0.8$(m).

The cylinder pressures measured by the sensors during the excavation process are shown in Fig. 16. The soil resistive forces are presented in Fig. 17 (a). A clear separation exists between the different excavation stages in the picture because the bucket movement has paused between different stages during the experiment. The force data during penetration is used to identify the soil parameters. Furthermore, the improved FEE model is used to predict the soil–bucket interaction force during cutting. The soil parameters obtained by fuzzy identification are presented in Table 5. The simulated soil forces compared with the measured forces during cutting are shown in Fig. 17 (b), and the errors are reported in Fig. 17 (c). The maximum error is 344 N (12.8%), and the root mean square error (RMSE) is 153 N. As the sand is one of the typical soils in the fuzzy rule library, the parameter identification results are very close to the actual soil parameters, and the predicted forces are also in good agreement with the measured forces during cutting.

TABLE 5. Real value and an estimation value of soil parameters.

Parameter and symbol	Real value	Estimation value
Hardness (kd)	/	0.512
Density (γ)	1753kg/m^3	1733 kg/m^3
Cohesion (c)	13.3kPa	12.1kPa
Bucket-soil friction angle (δ)	28.4°	27.7°
Internal friction angle (ϕ)	32.0°	30.7°

C. TEST 2 (SOIL WITH UNKNOWN PARAMETERS)

Aside from testing the soil with known parameters in the soil box, field experiments were conducted to further verify the effectiveness of the proposed framework. The experimental

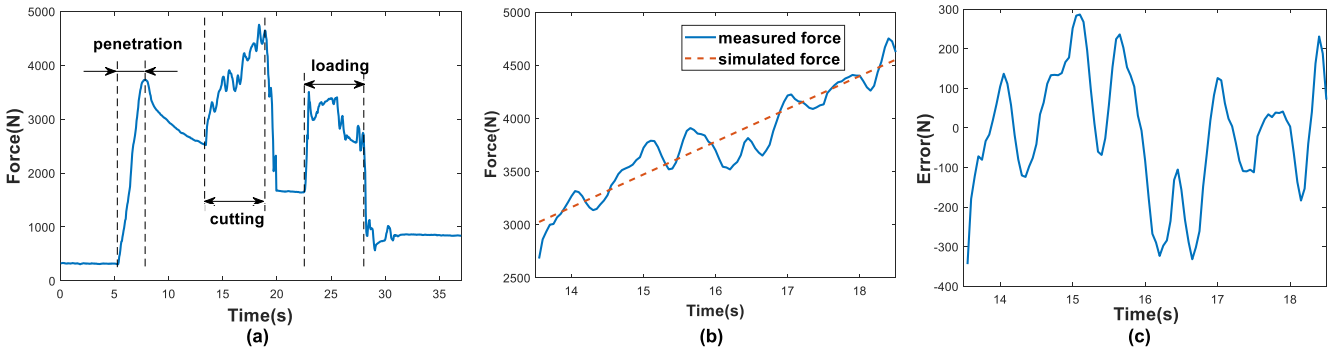

FIGURE 17. Simulated and measured soil forces during Test 1 (a) Measured force. (b) Comparison. (c) Error.

FIGURE 18. Field experiment site.

site is shown in Fig. 18, where the soil properties are the same. This condition is different from the soil box experiment in Test 1, where it is convenient to use instruments to obtain accurate parameters of the test soil. As the soil properties suffer after excavation, and obtaining the entire soil bulk for parameter testing is difficult, the field experiment can only estimate the parameters according to the soil conditions on the site [20], which are inaccurate.

TABLE 6. Estimation parameters of tested soil.

Parameter and symbol	Estimation value
Hardness (kd)	0.252
Density (γ)	1619.4 kg/m^3
Cohesion (c)	1.2kPa
Bucket-soil friction angle (δ)	20.3°
Internal friction angle (ϕ)	23.4°

The average values of cylinder pressures measured by sensors in multiple experiments are shown in Fig. 19, and the average digging forces are shown in Fig. 20(a). The results of fuzzy identification are reported in Table 6. Although obtaining the specific parameters of the excavated soil to analyze the accuracy of the fuzzy identification method during field experiments is difficult, the comparison between the predicted forces and measured forces can prove the effectiveness of the entire framework. We are more concerned about the accuracy of the force prediction during the cutting process rather than the specific parameters of the soil. The comparison of the simulated soil forces and measured forces is presented in Fig. 20(b), and the errors are shown in Fig. 20(c). The maximum error is 313N (22%), and the RMSE is 166 N.

The results of Tests 1 and 2 show that the fuzzy identification and force prediction methods proposed in this paper can accurately predict the soil-bucket interaction forces during the cutting stage. Whether the tested soil is in a soil box or a field site, the predicted forces and measured forces had a good consistency. Compared with the traditional way [13]–[16] of predicting after identifying which needs at least two excavations, the proposed method has better usability, flexibility, and real-time performance. In the research of Kim *et al.* [10], before predicting resistance, a test excavation was required to identify soil parameters, while a complete digging process usually cost more than 10 seconds. Furthermore, at least two excavations are needed to establish the equations of soil parameter identification in [8], and only two parameters can be identified. However, at least four soil parameters are needed to predict resistance by using the FEE model. It will undoubtedly take more time to obtain other soil parameters. Besides, the proposed method can continuously update soil parameters during each excavation. Therefore, the proposed method can perform soil parameter identification and prediction of excavation resistance during one excavation, which brings the advantage that we can predict soil resistive forces and plan the optimal excavation trajectory according to the soil properties. In general, under the premise of meeting the requirements of engineering application accuracy, the proposed method can identify soil parameters in a dynamic and timely manner, which is beneficial to the application in engineering.

The accuracy of the resistance prediction result of Test 1 is significantly better than that of Test 2 because the soil tested in Experiment 1 is one of the types in the fuzzy rule database, and the soil parameters of Test 2 are unknown and not in the database. The proposed methods are limited by the amount

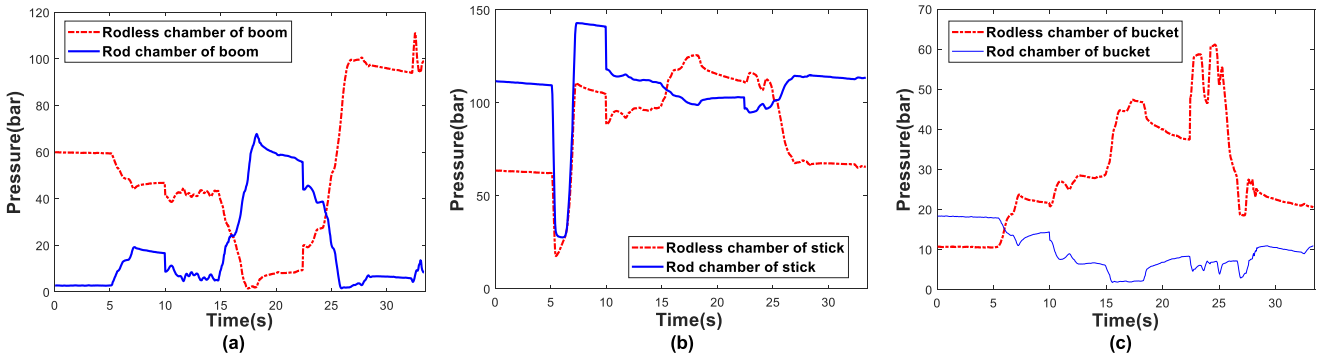

FIGURE 19. Cylinder pressures during Test 2 (a) Boom. (b) Stick. (c) Bucket.

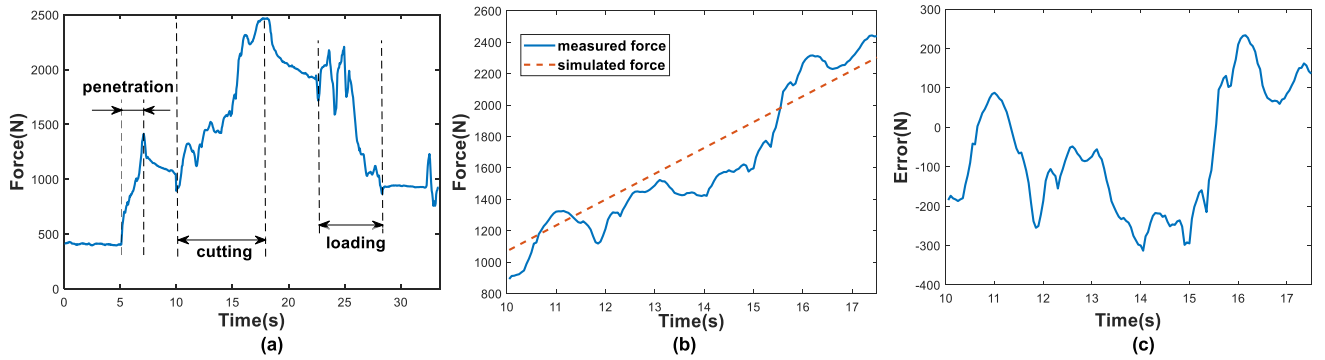

FIGURE 20. Simulated and measured soil forces during Test 2 (a) Measured force. (b) Comparison. (c) Error.

of soil in the fuzzy rule database. The more categories of soil we test, the more abundant the soil database, and the more accurate the results of the force prediction, which points the way to our next work: finding more categories of soil for testing and enriching our soil databases. However, due to the limitations of experimental conditions, obtaining many different types of soil in a short time is difficult. The finite element simulation methods [29], [30] for obtaining the soil-bucket interaction force will be used in our next study.

VI. CONCLUSION

The problem of identifying soil parameters efficiently and rapidly on earth-moving tasks is located and settled by the new method established in this study. Real-time estimation of soil parameters on penetration is built for excavation resistance prediction and operation trajectory regulation. Five typical soil types were first prepared after softness, and then a large number of experiments on penetration were conducted. The resistance databases were built to take advantage of the dynamic model, which is to obtain the action between the soil and bucket. Furthermore, to predict the resistance on penetration, a fuzzy estimation strategy was presented to obtain soil parameters according to the characteristics of penetrating resistances. The refined FEE model was also introduced to describe soil-bucket interaction forces and thus predict the penetration resistance. The soil box and field experiments are conducted to manifest the validity of the proposed method.

The main contribution of this paper is to complete parameter identification and resistance prediction in a one-time excavation. Unlike the traditional prediction-after-identification method that needs at least two excavations, the proposed theory segments one process into three parts. Soil parameters can be identified through soil force characteristic analysis during the penetration stage while predicting the soil-bucket interaction forces during the cutting stage. The newly designed fast soil parameter identification and resistance prediction method will dynamically identify soil parameters and predict excavation resistance with greater accuracy if the soil databases are larger. The method is also more applicable to soil variety and practical application.

High accuracy of parameter identification and the comparatively exact value of prediction resistance are achieved when properties of soil are acquired. For the experiments without these properties, the error occurs between the prediction resistance and actual resistance because of the limitation of the soil sample amount. Only five types of typical soil samples were collected, which was not large enough to predict digging resistance. Thus, expansion is needed on soil databases to ensure higher accuracy in resistance prediction. In addition, a dynamic trajectory plan scheme based on it will be discussed in our next study.

REFERENCES

[1] K. Kim, M. Kim, D. Kim, and D. Lee, "Modeling and velocity-field control of autonomous excavator with main control valve," *Automatica*, vol. 104, pp. 67–81, Jun. 2019.

[2] F. A. Bender, M. Mitschke, T. Bräunl, and O. Sawodny, "Predictive operator modeling for virtual prototyping of hydraulic excavators," *Autom. Construct.*, vol. 84, pp. 133–145, Dec. 2017.

[3] H. Feng, C. Yin, R. Li, W. Ma, H. Yu, D. Cao, and J. Zhou, "Flexible virtual fixtures for human-excavator cooperative system," *Autom. Construct.*, vol. 106, Oct. 2019, Art. no. 102897.

[4] D. Jud, P. Leemann, S. Kerscher, and M. Hutter, "Autonomous free-form trenching using a walking excavator," *IEEE Robot. Autom. Lett.*, vol. 4, no. 4, pp. 3208–3215, Oct. 2019.

[5] B. Zhang, S. Wang, Y. Liu, and H. Yang, "Research on trajectory planning and autodig of hydraulic excavator," *Math. Problems Eng.*, vol. 2017, May 2017, Art. no. 7139858.

[6] X. Zhang, S. Qiao, L. Quan, and L. Ge, "Velocity and position hybrid control for excavator boom based on independent metering system," *IEEE Access*, vol. 7, pp. 71999–72011, 2019.

[7] C. Tan, Y. Zweiri, K. Althoefer, and L. Seneviratne, "Online soil-bucket interaction identification for autonomous excavation," in *Proc. IEEE Int. Conf. Robot. Autom.*, Jan. 2006, pp. 3576–3581.

[8] C. Tan, Y. Zweiri, K. Althoefer, and L. Seneviratne, "Online soil parameter estimation scheme based on Newton-Raphson method for autonomous excavation," *IEEE/ASME Trans. Mechatronics*, vol. 10, no. 2, pp. 221–229, Apr. 2005.

[9] N. Bennett, A. Walawalkar, M. Heck, and C. Schindler, "Integration of digging forces in a multi-body-system model of an excavator," *Proc. Inst. Mech. Eng. K, J. Multi-Body Dyn.*, vol. 230, no. 2, pp. 159–177, Jun. 2016.

[10] Y. B. Kim, J. Ha, H. Kang, P. Y. Kim, J. Park, and F. Park, "Dynamically optimal trajectories for earthmoving excavators," *Autom. Construct.*, vol. 35, pp. 568–578, Nov. 2013.

[11] A. Gurko, O. Sergiyenko, J. I. N. Hipólito, I. Kirichenko, V. Tyrsa, and J. D. D. S. Lopez, "Guaranteed control of a robotic excavator during digging process," in *Proc. 12th Int. Conf. Informat. Control, Autom. Robot.*, vol. 2, Jul. 2015, pp. 52–59

[12] S. Dadhich, U. Bodin, and U. Andersson, "Key challenges in automation of Earth-moving machines," *Autom. Construct.*, vol. 68, pp. 212–222, Aug. 2016.

[13] O. Luengo, S. Singh, and H. Cannon, "Modeling and identification of soil-tool interaction in automated excavation," in *Proc. . IEEE/RSJ Int. Conf. Intell. Robots Syst. Innov. Theory, Pract. Appl.*, vol. 3, Nov. 2002, pp. 1900–1906.

[14] W. J. Hong, "Modeling, estimation, and control of robot-soil interactions," Ph.D. dissertation, Dept. Mech. Eng., Massachusetts Inst. Technol., Cambridge, MA, USA, 2001.

[15] K. Althoefer, C. Tan, Y. Zweiri, and L. Seneviratne, "Hybrid soil parameter measurement and estimation scheme for excavation automation," *IEEE Trans. Instrum. Meas.*, vol. 58, no. 10, pp. 3633–3641, Oct. 2009.

[16] A. R. Reece, "The fundamental equation of earthmoving mechanics," *Proc. Inst. Mech. Engrs.*, vol. 179, pp. 1964–1965, 1965.

[17] E. McKyes, *Soil Cutting and Tillage*. New York, NY, USA: Elsevier, 1985.

[18] X. Zeng, L. Burnoski, J. Agui, and A. Wilkinson, "Calculation of excavation force for ISRU on lunar surface," in *Proc. 45th AIAA Aerosp. Sci. Meeting Exhibit*, Jan. 2007, p. 1474.

[19] B. Park, "Development of a virtual reality excavator simulator: A mathematical model of excavator digging and a calculation methodology," M.S. thesis, Virginia Polytechnic Inst. State Univ., Blacksburg, VA, USA, 2002.

[20] Z. Zou, J. Chen, and X. Pang, "Task space-based dynamic trajectory planning for digging process of a hydraulic excavator with the integration of soil–bucket interaction," *Proc. Inst. Mech. Eng. K, J. Multi-Body Dyn.*, vol. 233, no. 3, pp. 598–616, Sep. 2019.

[21] S. Blouin, A. Hemami, and M. Lipsett, "Review of resistive force models for earthmoving processes," *J. Aerosp. Eng.*, vol. 14, no. 3, pp. 102–111, Jul. 2001.

[22] S. Singh, "Learning to predict resistive forces during robotic excavation," in *Proc. IEEE Int. Conf. Robot. Autom.*, vol. 2, Nov. 2002, pp. 2102–2107.

[23] A. N. Zelenin, V. I. Balovnev, I. P. Kerov, *Machines for Moving the Earth*. New Delhi, India: Amerind, 1985.

[24] R. S. Fowkes, D. E. Frisque, and W. G. Pariseau, "Materials handling research: Penetration of selected/granular materials by wedgeshaped tools," in *Report Investigations*, vol. 7739. Washington, DC, USA: Search Results Web results United States Bureau of Mines, 1973.

[25] H. Deng, Y. Zhang, and X.-G. Duan, "Wavelet transformation-based fuzzy reflex control for prosthetic hands to prevent slip," *IEEE Trans. Ind. Electron.*, vol. 64, no. 5, pp. 3718–3726, May 2017.

[26] X.-G. Duan, H. Deng, and H.-X. Li, "A saturation-based tuning method for fuzzy PID controller," *IEEE Trans. Ind. Electron.*, vol. 60, no. 11, pp. 5177–5185, Nov. 2013.

[27] W. Y. Yang, W. W. Cao, T. S. Chung, M. John, *Applied Numerical Methods Using MATLAB*. Hoboken, NJ, USA: Wiley, 2004, pp. 145–149.

[28] B. Xi, M. Jiang, L. Cui, J. Liu, and H. Lei, "Experimental verification on analytical models of lunar excavation," *J. Terramechanics*, vol. 83, pp. 1–13, Jun. 2019.

[29] C. Coetzee and D. Els, "The numerical modelling of excavator bucket filling using DEM," *J. Terramechanics*, vol. 46, no. 5, pp. 217–227, Oct. 2009.

[30] S. F. Azam and P. Rai, "Finite element-based simulation and analysis of dragline bucket in static and dynamic loading condition," *Current Sci.*, vol. 116, no. 4, p. 612, Jan. 2020.

YUMING ZHAO received the Ph.D. degree in mechanical engineering from Central South University, China, in 2019. He is currently the Director of the Department of Special Equipment Design, Sunward Intelligent Equipment Company, Ltd., China. He is mainly engaged in the control and automation research of electro-hydraulic integrated systems.

JIAN WANG received the B.E. degree from the School of Mechanical and Electrical Engineering, Central South University, Changsha, China, where he is currently pursuing the Ph.D. degree. His current research interests include system modeling, intelligent control, and learning.

YI ZHANG received the B.E. and Ph.D. degrees from the School of Mechanical and Electrical Engineering, Central South University, China. He is currently a Postdoctoral Fellow with the School of Mechanical and Electrical Engineering, Central South University. He is also a Lecturer with the School of Mechanical and Electrical Engineering, Changsha University, China. His current research interests include mechanism design, system modeling, and control.

CHAO LUO received the Ph.D. degree in engineering from The Institute of Vibration, Shock and Noise, Shanghai Jiao Tong University, China. He is currently a Research Fellow with the Department of Special Equipment Design, Sunward Intelligent Equipment Company, Ltd., China. He is specialized in mechanism design, system modeling, and control.